Available online www.jsaer.com

***Journal of Scientific and Engineering Research*, 2018, 5(9):276-288**

Research Article

ISSN: 2394-2630
CODEN(USA): JSERBR

Improving Availability of Transit Capacity by the Hybrid Optimization Method

Mathurin GOGOM[1], Mavie MIMIESSE[2], Germain NGUIMBI[2], Désiré LILONGA-BOYENGA[2]

Laboratoire de Génie Electrique et Electronique, Ecole Nationale Supérieure Polytechnique, Université Marien Ngouabi, Brazzaville, Congo

Abstract In this paper, we present a hybrid optimization method for calculating the Available Transporter Capacitance (ATC) between interconnected zones, based on genetic algorithms and Advanced Power Flow. Genetic algorithms optimize the location of SVCs at nodes, while Advanced Power Flow is used for the calculation of load distribution by the Newton Raphson method including SVCs considered as susceptances or variable thyristor angles. This study makes it possible to increase the capacity of power transit between interconnected zones.

Keywords Hybrid Optimization, ATC, Genetic Algorithm, Advanced Compensation, Power Flow, SVCs

1. Introduction

Mesh electrical power networks, subject to often undesirable power loops between interconnected zones, suffer line overload, voltage stability problems and in all cases of them an increase in losses. Traditional or traditional means of control and management of networks (adjustable load transformer, phase-shift transformers, series or parallel compensators switched by circuit-breakers, modification of production instructions, change of network topology and action on the excitation of generators) could prove to be too slow and insufficient in the future to respond effectively to network disruptions, particularly in the light of new constraints. It will therefore be necessary to complete their action by implementing power electronics devices with short response times known as Flexible Alternative Current Transmission Systems (FACTS) for network control and management [1] and SVCs [2].

Mesh electrical power networks, often subject to power loops The development of FACTS devices has opened new perspectives for a more efficient network operation by continuous and rapid action on the various parameters (phase shift, voltage, impedance). Thus, the power transits will be better controlled and the tensions better regulated which will increase the voltage stability margins and tend towards the thermal limits of the lines. Maintaining the balance between production and consumption then requires continuous monitoring of the system to ensure the quality of service (driving problem), guarantee its safety (protection problem) and stability (adjustment problem).

Because of network mesh, multiple FACTS can be used to improve voltage stability and transit capacity between interconnected zones. For economic reasons, it is not often easy to place the FACTS at each point of disruption. For this purpose, the location of these FACTS must be optimized.

Thus, in this study, we examine the problem of SVCs optimal placement to compensate reactive power and solve the problem of voltage instability in order to increase the capacity of power transmission lines. To achieve this goal, we use modern techniques of reactive power compensation based on the use of FACTS devices such as SVC. For this purpose, we will design a hybrid optimization algorithm linking genetic algorithms and advanced power flow.

The application of this approach on the Congolese power grid is presented to solve low transit capacity and Joule losses problems.

2. Theoretical study

The improvement of the available transit capacity is based on the compensation of the reactive power. Thus, there is the conventional compensation that uses the electromechanical devices and advanced compensation that is the subject of this study.

2.1. Advanced compensation

Faced with power transmission problems, the American company EPRI (Electric Power Research Institute) launched, in 1988, a project to study FACTS systems in order to better control the transit of power in power lines. The FACTS concept gathers all power electronics-based devices that improve the operation of electrical power network. The technology of these systems provides a higher speed than conventional electromechanical systems. FACTS devices can be classified into three categories [1-5]: parallel compensators; series compensators and hybrid compensators (series - parallel).

Advanced compensation using power electronics-based devices makes it possible to increase the transit capacity of the interconnection lines in order to predict the available transit capacity.

2.2. Calculation of the available transit capacity

Available Transfer Capacity (ATC) is a criterion for the fluidity of electricity networks in a deregulated electricity market environment. The available transfer capacity is the projected active power intended to satisfy future transactions in a liberal electricity market system. It is given by [8]:

ATC = TTC- ETC – TRM - CBM. (1)

Where the quantities:

- TTC (Total Transfer Capacity) is the maximum power whose transfer does not cause violations of the thermal limits and the stability of the electrical networks;
- ETC (Existing Transmission Commitment) is the power transited in accordance with the commitment in force between two interconnected zones;
- TRM (Transmission Reliability Margin) is the transfer capability required to ensure that the interconnected network is secure against system uncertainties [8];
- CBM (Capacity of Benefit Margin) is the transfer capacity of the reserved charges by the serving entities, which is necessary to guarantee access to the production in order to satisfy the reliability requirements [8].

The TTC and ETC calculations result from the load distribution calculation based on the system of equations at the network nodes [3]; [7] and [9]:

$$\begin{cases} P_i = Y_{ii}V_i^2\cos(\alpha_{ii}) + V_i\sum_{\substack{i=1\\k\neq 1}}^{n} Y_{ik}V_k\cos(\varphi_i-\varphi_k-\alpha_{ik}) \\ Q_i = Y_{ii}V_i^2\sin(\alpha_{ii}) + V_i\sum_{\substack{i=1\\k\neq 1}}^{n} Y_{ik}V_k\sin(\varphi_i-\varphi_k-\alpha_{ik}) \end{cases} \quad (2)$$

where the quantities P_i *and* Q_i are respectively the active and reactive powers injected or absorbed at node i with i = 1 to n; V_i *and* V_k are the voltage modules at nodes i and k with i = 1 to n and k = 2 to n;φ_i and φ_k are respectively the voltage phases at the nodes i and k; Y_{ii} and Y_{ik} are respectively the admittances incident to the node i then α_{ii} and α_{ik} are respectively the arguments of these admittances incident.

This system of equations can be solved using several methods developed in the literature [6, 7], including the Newton Raphson method which consists in linearizing this system of nonlinear equations and transcribing it in the form of following matrix equation:

$$\begin{bmatrix} \Delta P_1 \\ \Delta P_2 \\ \vdots \\ \Delta P_i \\ \Delta Q_1 \\ \Delta Q_2 \\ \vdots \\ \Delta Q_i \end{bmatrix} = \begin{bmatrix} \frac{\partial P_1}{\partial V_1} & \frac{\partial P_1}{\partial V_2} & \cdots & \frac{\partial P_1}{\partial V_i} & \frac{1}{V}\frac{\partial P_1}{\partial \varphi_1} & \frac{1}{V}\frac{\partial P_1}{\partial \varphi_2} & \cdots & \frac{1}{V}\frac{\partial P_1}{\partial \varphi_i} \\ \frac{\partial P_2}{\partial V_1} & \frac{\partial P_2}{\partial V_2} & \cdots & \frac{\partial P_2}{\partial V_i} & \frac{1}{V}\frac{\partial P_2}{\partial \varphi_1} & \frac{1}{V}\frac{\partial P_2}{\partial \varphi_2} & \cdots & \frac{1}{V}\frac{\partial P_2}{\partial \varphi_i} \\ \vdots & \vdots & \ddots & \vdots & \vdots & \vdots & \ddots & \vdots \\ \frac{\partial P_i}{\partial V_1} & \frac{\partial P_i}{\partial V_2} & \cdots & \frac{\partial P_i}{\partial V_i} & \frac{1}{V}\frac{\partial P_i}{\partial \varphi_1} & \frac{1}{V}\frac{\partial P_i}{\partial \varphi_1} & \cdots & \frac{1}{V}\frac{\partial P_i}{\partial \varphi_i} \\ \frac{\partial Q_1}{\partial V_1} & \frac{\partial Q_1}{\partial V_2} & \cdots & \frac{\partial Q_1}{\partial V_i} & \frac{1}{V}\frac{\partial Q_1}{\partial \varphi_1} & \frac{1}{V}\frac{\partial Q_1}{\partial \varphi_2} & \cdots & \frac{1}{V}\frac{\partial Q_1}{\partial \varphi_i} \\ \frac{\partial Q_2}{\partial V_1} & \frac{\partial Q_2}{\partial V_2} & \cdots & \frac{\partial Q_2}{\partial V_i} & \frac{1}{V}\frac{\partial Q_2}{\partial \varphi_1} & \frac{1}{V}\frac{\partial Q_2}{\partial \varphi_2} & \cdots & \frac{1}{V}\frac{\partial Q_2}{\partial \varphi_i} \\ \vdots & \vdots & \ddots & \vdots & \vdots & \vdots & \ddots & \vdots \\ \frac{\partial Q_i}{\partial V_1} & \frac{\partial Q_i}{\partial V_2} & \cdots & \frac{\partial Q_i}{\partial V_i} & \frac{1}{V}\frac{\partial Q_i}{\partial \varphi_1} & \frac{1}{V}\frac{\partial Q_i}{\partial \varphi_1} & \cdots & \frac{1}{V}\frac{\partial Q_i}{\partial \varphi_i} \end{bmatrix} \begin{bmatrix} \frac{\Delta V_1}{V} \\ \frac{\Delta V_2}{V} \\ \vdots \\ \frac{\Delta V_i}{V} \\ \Delta \varphi_1 \\ \Delta \varphi_2 \\ \vdots \\ \Delta \varphi_i \end{bmatrix} \quad (3)$$

2.3. Hybrid optimization method

The hybrid optimization method groups together the genetic algorithms whose functionalities give it optimization methods based on the optimal placement of SVC devices whose parameter is to optimize the location. Newton Raphson's advanced method, including SVCs, optimizes the susceptance of the thermistors' SVC, the node voltages, the transit capacitances and the Joule losses.

2.3.1. Genetic algorithm

This method is selected because of its convergence rapidity and accuracy of the results compared to other metaheuristic methods [3]. In this subsection, we describe the different stages of genetic algorithms working.

2.3.1.1. Initial population and coding

The initial population that constitutes all the configurations of network is generated in a random manner. Its size results from a compromise between the calculation time, the number of variables to be optimized and the quality of the populations found. It is advisable to increase the size in order to promote the intensification and diversification of individuals or configurations.

The coding of individuals is an important parameter of the method. Individuals are represented as chains containing characters or (genes) of a certain alphabet. The coding must be adapted to the problem in order to limit the size of the search space by producing valid solutions as often as possible when applying the search operators. The representation must be such that the search operators are efficient to reproduce the solutions sought with a good probability.

In this work, we use the binary coding in which each solution is represented by a string of 0 or 1 called bit. The genetic algorithm often uses this representation when dealing with complex structures. The number of bits is equal to the number of nodes of instability of the network in voltage, that is to say the nodes to which the SVC can be connected. The string takes the character or (alphabet) 0 when the SVC is not connected and 1 when connected. Each character corresponds to a number of the instability node.

2.3.1.2. Evaluation

Evaluation is the most expensive part algorithm in computation time because it needs the results of the advanced load distribution calculation. Once the initial population is created, each individual (configuration) is evaluated against the optimization objective considered. In order to find an optimal location for the SVCs, the evaluation consists of the losses calculation in the network using the advanced Newton Raphson method in order to deduce the evaluation function. For our case, the evaluation function, called fitness function is given by [3]:

$$f_{it_i} = \frac{1}{p_m + \frac{x_{cali} - x_{min}}{x_{max} - x_{min}} p_c} \quad (4)$$

where p_m is the mutation probability, p_c the crossover probability, x_{cali} the joule losses calculated for each configuration, x_{max} the upper limit of the joule losses in the networks and x_{min} the lower limit of joule losses in the network.

According to this formulation, the fitness function can take values between 0 and 10 for the best configurations, and greater than 10 for the less good ones. The population at a given time of the algorithm is called generation. Once the generation is evaluated, individuals are ranked according to the value of their fitness function.

2.3.1.3. Selection

The selection of individuals for the intermediate generation is carried out, in our case, by the biased roulette draw on which each individual has a share proportional to his fitness function. This selection technique allows quality individuals to be part of the next generation, but it also avoids premature convergence of the algorithm. It is necessary to maintain sufficient genetic diversity in the population to ensure genes that can be subsequently. Indeed, any individual can transmit to his descendant's genes that, when combined with others, may reveal interesting.

2.3.1.4. Crossing

After selection, the crossing of two individuals to give two children can occur with a probability between 0.8 and 1. In this research work, the multipoint cross is applied. For this, some points are drawn randomly, and between these points, the elements (SVC) of the two solutions (configurations) are exchanged. As mentioned in [11], two FACTS controllers of the same type cannot be inserted in the same element of the network (branch or node). However, the crossing operator can give rise to such a situation. Similarly, as in this study, only SVCs are used, so the crossover operator should not replace one SVC with another SVC (bit 1 with bit 1, but bit 1 with bit 0). To overcome this, a code is established for this purpose. The procedure is repeated until a SVC is connected to each voltage instability node. An example of a multipoint crossover of two individuals is shown in Figure 1.

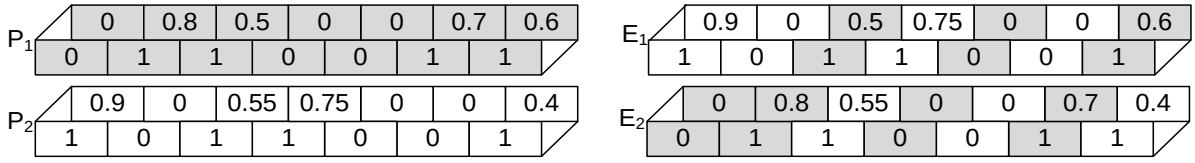

Figure 1: multipoint crossing of both parents

This example represents the case of eight nodes of voltage instability. However, there are four SVCs to be optimally placed so as to obtain voltage stability, minimum joule losses and better fluidity of the transport network.

2.3.1.5. Mutation

In our case, the mutations can take place on the characters of the two chains (the locations and the susceptances or angles of priming) representing a solution. The effect of the mutation results in a change of value of the selected element. The new value is randomly drawn from the possible values. The mutation on several elements of each of the two chains is illustrated in Figure 2.

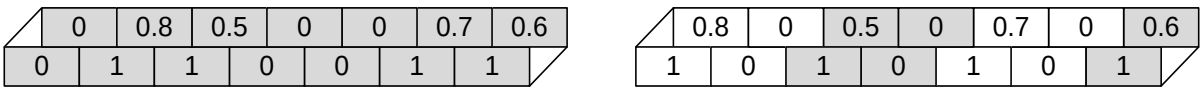

Figure 2: mutation of characters of two chains

A specific mutation probability is applied to each parameter:

p_{me} for locations; p_{mv} for the set values of the susceptances or angles of initiation. These probabilities vary over generations. They increase to favor diversification when the population tends to be represented by only a few dominant individuals. The probability of mutation can be between 0.01 and 0.2. The general functioning of genetic algorithms is given in Figure 3[3].

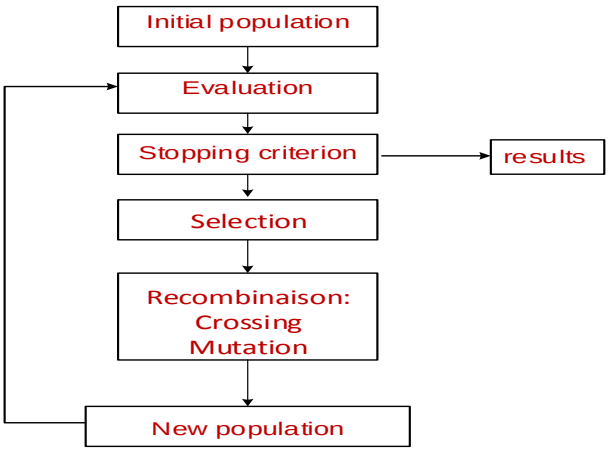

Figure 3: functioning of genetic algorithms

1.3.2. Newton Raphson method including FACTS

Two modelling approaches are used to represent and implement the static reactive power compensator (SVC) [3] and [9]: The approach, known as classical or conventional method of Newton Raphson including FACTS controllers based on the representation and the implementation of the SVC like a generator behind a fixed inductor. The unified approach of modelling the SVC controller, known as Newton Raphson's advanced method including FACTS controllers, takes into account the combination of state variables describing the FACTS controllers in this case the SVC and the state variables describing the network in the same repository. This approach keeps the quadratic convergence characteristics.

It combines the state variables of the electrical network and those of the SVCs into a single system of equations defined by [3]:

$$\begin{cases} f(X,U)=0 \\ g(X,U)=0 \end{cases} \quad (5)$$

where X represents the state variables (modules and voltage phases at the nodes of the electrical network), U represents the state variables of the SVC controllers (susceptances or angles of initiation), $f(X,U)=0$ represents the Active power equations at the nodes of the electrical network and $g(X,U)=0$ represents the reactive power equations at the nodes of the electrical network. The increase of the dimensions of the Jacobian matrix, compared to the network without SVC, is almost proportional to the number of SVCs. In the following we will retain the advanced method of Newton Raphson including FACTS controllers.

1.3.3. Advanced Newton Raphson method including SVCs

Newton Raphson's advanced method including SVCs is based on two models described as follows [9]:

1.3.3.1. Variable susceptance model

The SVC controller is represented by the model of figure 4. According to this model, the current called by the controller SVC is given by:

$$\underline{\boldsymbol{I}}_{\boldsymbol{SVC}} = \boldsymbol{iB}_{\boldsymbol{SVC}}\underline{\boldsymbol{V}}_{\boldsymbol{k}} \quad (6)$$

And the reactive power called by the SVC controller, which is also the reactive power injected at the node k is:

$$\boldsymbol{Q}_{\boldsymbol{SVC}} = \boldsymbol{Q}_{\boldsymbol{k}} = -\boldsymbol{V}_{\boldsymbol{k}}^{\boldsymbol{2}}\boldsymbol{B}_{\boldsymbol{SVC}} \quad (7)$$

From this non-linear equation, we obtain a linearized equation such as:

$$\begin{pmatrix} \Delta \boldsymbol{P}_{\boldsymbol{k}} \\ \Delta \boldsymbol{Q}_{\boldsymbol{k}} \end{pmatrix}^{\boldsymbol{i}} = \begin{pmatrix} \boldsymbol{0} & \boldsymbol{0} \\ \boldsymbol{0} & \boldsymbol{Q}_{\boldsymbol{k}} \end{pmatrix}^{\boldsymbol{i}} \begin{pmatrix} \Delta \boldsymbol{\theta} \\ \frac{\Delta \boldsymbol{B}_{\boldsymbol{SVC}}}{\boldsymbol{B}_{\boldsymbol{SVC}}} \end{pmatrix}^{\boldsymbol{i}} \quad (8)$$

At the end of the ith iteration, the BSVC variable susceptance is updated according to the total susceptance of the SVC controller, necessary to maintain the module of the voltage at the node at a specified value.

$$\boldsymbol{B}_{\boldsymbol{SVC}}^{(\boldsymbol{i})} = \boldsymbol{B}_{\boldsymbol{SVC}}^{(\boldsymbol{i-1})} + \left(\frac{\Delta \boldsymbol{B}_{\boldsymbol{SVC}}}{\boldsymbol{B}_{\boldsymbol{SVCt}}}\right)^{\boldsymbol{i}} (\boldsymbol{B}_{\boldsymbol{SVC}})^{(\boldsymbol{i-1})} \quad (9)$$

Once the level of compensation is reached, then the firing angle of the thyristor can be calculated. Moreover, the additional calculation needs an iterative solution, since the susceptance of the SVC controller and the priming angle of the thyristor are linked by a non-linear equation

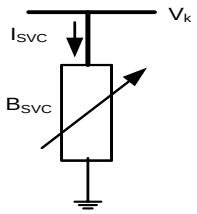

Figure 4: model of variable shunt susceptance

1.3.3.2. Variable priming angle model

This model consists in managing of the thyristor priming angle ($\boldsymbol{\alpha_{SVC}}$) as a state variable in the formulation of Newton Raphson's advanced method including FACTS.

The susceptance of the SVC controller used in equation (9) makes it possible to formulate the reactive power at node k such that [9]:

$$\boldsymbol{Q_k = -\frac{V_k^2}{X_C X_L}\left\{X_L - \frac{X_C}{\pi}[2(\pi - \alpha_{SVC}) + \sin(2\alpha_{SVC})]\right\}} \quad (10)$$

The linearized form of the SVC controller equation is:

$$\begin{pmatrix}\Delta \boldsymbol{P_k}\\ \Delta \boldsymbol{Q_k}\end{pmatrix}^{\boldsymbol{i}} = \begin{pmatrix}\boldsymbol{0} & \boldsymbol{0}\\ \boldsymbol{0} & \boldsymbol{\frac{2V_k^2}{X_C X_L}[\cos(2\alpha_{SVC}) - 1]}\end{pmatrix}^{\boldsymbol{i}} \begin{pmatrix}\Delta \boldsymbol{\theta_k}\\ \Delta \boldsymbol{\alpha_{SVC}}\end{pmatrix}^{\boldsymbol{i}} \quad (11)$$

At the end of the ith iteration, the variable boot angle of SVC α_svc is updated and we have:

$$\alpha_{SVC}^{(i)} = \alpha_{SVC}^{(i-1)} + \Delta\alpha_{SVC}^{(i)} \quad (12)$$

By including the SVCs, equation (3), given in matrix form, becomes:

$$\begin{bmatrix}\Delta P_1\\ \Delta P_2\\ \vdots\\ \Delta P_i\\ \Delta Q_1\\ \Delta Q_2\\ \vdots\\ \Delta Q_i\\ \Delta Q_{SVC1}\\ \Delta Q_{SVC2}\\ \vdots\\ \Delta Q_{SVCi}\end{bmatrix} = \begin{bmatrix}
\frac{\partial P_1}{\partial V_1} & \frac{\partial P_1}{\partial V_2} & \cdots & \frac{\partial P_1}{\partial V_i} & \frac{1}{V}\frac{\partial P_1}{\partial \varphi_1} & \frac{1}{V}\frac{\partial P_1}{\partial \varphi_2} & \cdots & \frac{1}{V}\frac{\partial P_1}{\partial \varphi_i} & \frac{B_{SVC}}{V}\frac{\partial P_1}{\partial B_{SVC1}} & \frac{B_{SVC}}{V}\frac{\partial P_1}{\partial B_{SVC2}} & \cdots & \frac{B_{SVC}}{V}\frac{\partial P_1}{\partial B_{SVCi}}\\
\frac{\partial P_2}{\partial V_1} & \frac{\partial P_2}{\partial V_2} & \cdots & \frac{\partial P_2}{\partial V_i} & \frac{1}{V}\frac{\partial P_2}{\partial \varphi_1} & \frac{1}{V}\frac{\partial P_2}{\partial \varphi_2} & \cdots & \frac{1}{V}\frac{\partial P_2}{\partial \varphi_i} & \frac{B_{SVC}}{V}\frac{\partial P_2}{\partial B_{SVC1}} & \frac{B_{SVC}}{V}\frac{\partial P_2}{\partial B_{SVC2}} & \cdots & \frac{B_{SVC}}{V}\frac{\partial P_2}{\partial B_{SVCi}}\\
\vdots & \vdots & \ddots & \vdots & \vdots & \vdots & \ddots & \vdots & \vdots & \vdots & \ddots & \vdots\\
\frac{\partial P_i}{\partial V_1} & \frac{\partial P_i}{\partial V_2} & \cdots & \frac{\partial P_i}{\partial V_i} & \frac{1}{V}\frac{\partial P_i}{\partial \varphi_1} & \frac{1}{V}\frac{\partial P_i}{\partial \varphi_1} & \cdots & \frac{1}{V}\frac{\partial P_i}{\partial \varphi_i} & \frac{B_{SVC}}{V}\frac{\partial P_i}{\partial B_{SVC1}} & \frac{B_{SVC}}{V}\frac{\partial P_i}{\partial B_{SVC1}} & \cdots & \frac{B_{SVC}}{V}\frac{\partial P_i}{\partial B_{SVCi}}\\
\frac{\partial Q_1}{\partial V_1} & \frac{\partial Q_1}{\partial V_2} & \cdots & \frac{\partial Q_1}{\partial V_i} & \frac{1}{V}\frac{\partial Q_1}{\partial \varphi_1} & \frac{1}{V}\frac{\partial Q_1}{\partial \varphi_2} & \cdots & \frac{1}{V}\frac{\partial Q_1}{\partial \varphi_i} & \frac{B_{SVC}}{V}\frac{\partial Q_1}{\partial B_{SVC1}} & \frac{B_{SVC}}{V}\frac{\partial Q_1}{\partial B_{SVC2}} & \cdots & \frac{B_{SVC}}{V}\frac{\partial Q_1}{\partial B_{SVCi}}\\
\frac{\partial Q_2}{\partial V_1} & \frac{\partial Q_2}{\partial V_2} & \cdots & \frac{\partial Q_2}{\partial V_i} & \frac{1}{V}\frac{\partial Q_2}{\partial \varphi_1} & \frac{1}{V}\frac{\partial Q_2}{\partial \varphi_2} & \cdots & \frac{1}{V}\frac{\partial Q_2}{\partial \varphi_i} & \frac{B_{SVC}}{V}\frac{\partial Q_2}{\partial B_{SVC1}} & \frac{B_{SVC}}{V}\frac{\partial Q_2}{\partial B_{SVC2}} & \cdots & \frac{B_{SVC}}{V}\frac{\partial Q_2}{\partial B_{SVCi}}\\
\vdots & \vdots & \ddots & \vdots & \vdots & \vdots & \ddots & \vdots & \vdots & \vdots & \ddots & \vdots\\
\frac{\partial Q_i}{\partial V_1} & \frac{\partial Q_i}{\partial V_2} & \cdots & \frac{\partial Q_i}{\partial V_i} & \frac{1}{V}\frac{\partial Q_i}{\partial \varphi_1} & \frac{1}{V}\frac{\partial Q_i}{\partial \varphi_2} & \cdots & \frac{1}{V}\frac{\partial Q_i}{\partial \varphi_i} & \frac{B_{SVC}}{V}\frac{\partial Q_i}{\partial B_{SVC1}} & \frac{B_{SVC}}{V}\frac{\partial Q_i}{\partial B_{SVC2}} & \cdots & \frac{B_{SVC}}{V}\frac{\partial Q_i}{\partial B_{SVCi}}\\
\frac{\partial Q_{SVC1}}{\partial V_1} & \frac{\partial Q_{SVC1}}{\partial V_2} & \cdots & \frac{\partial Q_{SVC1}}{\partial V_i} & \frac{1}{V}\frac{\partial Q_{SVC1}}{\partial \varphi_1} & \frac{1}{V}\frac{\partial Q_{SVC1}}{\partial \varphi_2} & \cdots & \frac{1}{V}\frac{\partial Q_{SVC1}}{\partial \varphi_i} & \frac{B_{SVC}}{V}\frac{\partial Q_{SVC1}}{\partial B_{SVC1}} & \frac{B_{SVC}}{V}\frac{\partial Q_{SVC1}}{\partial B_{SVC2}} & \cdots & \frac{B_{SVC}}{V}\frac{\partial Q_{SVC1}}{\partial B_{SVCi}}\\
\frac{\partial Q_{SVC2}}{\partial V_1} & \frac{\partial Q_{SVC2}}{\partial V_2} & \cdots & \frac{\partial Q_{SVC2}}{\partial V_i} & \frac{1}{V}\frac{\partial Q_{SVC2}}{\partial \varphi_1} & \frac{1}{V}\frac{\partial Q_{SVC2}}{\partial \varphi_2} & \cdots & \frac{1}{V}\frac{\partial Q_{SVC2}}{\partial \varphi_i} & \frac{B_{SVC}}{V}\frac{\partial Q_{SVC2}}{\partial B_{SVC1}} & \frac{B_{SVC}}{V}\frac{\partial Q_{SVC2}}{\partial B_{SVC2}} & \cdots & \frac{B_{SVC}}{V}\frac{\partial Q_{SVC2}}{\partial B_{SVCi}}\\
\vdots & \vdots & \ddots & \vdots & \vdots & \vdots & \ddots & \vdots & \vdots & \vdots & \ddots & \vdots\\
\frac{\partial Q_{SVCi}}{\partial V_1} & \frac{\partial Q_{SVCi}}{\partial V_2} & \cdots & \frac{\partial Q_{SVCi}}{\partial V_i} & \frac{1}{V}\frac{\partial Q_{SVCi}}{\partial \varphi_1} & \frac{1}{V}\frac{\partial Q_{SVCi}}{\partial \varphi_2} & \cdots & \frac{1}{V}\frac{\partial Q_{SVCi}}{\partial \varphi_i} & \frac{B_{SVC}}{V}\frac{\partial Q_{SVCi}}{\partial B_{SVC1}} & \frac{B_{SVC}}{V}\frac{\partial Q_{SVCi}}{\partial B_{SVC2}} & \cdots & \frac{B_{SVC}}{V}\frac{\partial Q_{SVCi}}{\partial B_{SVCi}}
\end{bmatrix} \begin{bmatrix}\frac{\Delta V_1}{V}\\ \frac{\Delta V_2}{V}\\ \vdots\\ \frac{\Delta V_i}{V}\\ \Delta\varphi_1\\ \Delta\varphi_2\\ \vdots\\ \Delta\varphi_i\\ \frac{\Delta B_{SVC1}}{B_{SVC}}\\ \frac{\Delta B_{SVC2}}{B_{SVC}}\\ \vdots\\ \frac{\Delta B_{SVCi}}{B_{SVC}}\end{bmatrix}$$

1.3.4. Formulation of the optimization problem

In this work, we use many SVC devices. For this purpose, fuzzy logic [11] is used to control multiple SVC devices in use. Here, the two-step optimization is applied: the first is to optimize the locations and the setpoint values (boot angle or susceptance) of the SVCs, considered as state variables, the number and type of FACTS devices being known and the second step is to optimize the state variables of the electrical network.

To do this, the objective function is formulated to minimize Joule losses in the electrical network; the equality constraints are attached (the equations of the powers at the nodes which must obey the laws of Kirchhoff) and the constraints of inequality are also attached:

- the voltages at the nodes must not deviate sufficiently from the reference values;
- SVC generators and controllers must be operated close to their operating limits;
- the power transits in the lines must be close to thermal limits.

The purpose is to guarantee protected operations (absence of mutual influences between SVC devices and the failure to exceed the limits) and to solve the problem of increasing the transfer capacity of the power lines, making it possible to predict the capacity available to carry between interconnected areas.

Thus, the hybrid optimization problem can be formulated mathematically as follows:

minimize $f(X,U)$to deduce the best fitness function f_{it_i} and take into account the following sub constraints:

$$\begin{cases} g(X,U) = 0 \\ h(X,U) \leq 0 \end{cases} \quad (13)$$

where *X* is the state vector of the electrical network (modules and voltage phases at the nodes), *U* the vector representing the variables of the SVC controllers and the possible auxiliary variables, all considered as state variables and $f(X,U)$the objective function, representing the losses joule in the electrical network, determined by the branches' method.

Thus, the fitness function given by relation (14) makes it possible to evaluate and select the individuals necessary for recombination.

$$f_{it_i} = \frac{1}{p_m + \frac{f(X,U)_{cali} - f(X,U)_{min}}{f(X,U)_{max} - f(X,U)_{min}} p_c} \quad (14)$$

In this relation g (X, U) represents the equality constraints, corresponding to the power injection equations including those of the SVCs and h (X, U) the inequality constraints, expressing the limitations on the equipment in service (generators, lines and SVC):

For generators, these limits are expressed by:

$$Q_i^{min} \leq Q_i(V,U) \leq Q_i^{max} \quad (15)$$

where

$$Q_i^{min} - Q_i(V,U) \leq 0 \text{ and } Q_i(V,U) - Q_i^{max} \leq \quad (16)$$

where Qi is a function of the modules and voltage phases at the ith node and all neighbouring nodes.

If at the end of the calculation, or during the calculation, the production Qi comes to exceed the upper bound Q_i^{max}, one imposes:

$$Q_i(V,U) - Q_i^{max} = 0$$

Similarly, if production exceeds the lower bound Q_i^{min} , one imposes :

$$Q_i^{min} - Q_i(V,U) = 0$$

In both cases, the node of the PV type becomes PQ.

For lines, the power flows must not exceed 90% of their respective transfer capability. For each line, the following inequalities are valid:

$$S_{ik} \leq 0.9\, S_{ik}^{max} + \epsilon_{ik}\ ,\ 0 \leq \epsilon_{ik} \text{ and } S_{ik} \leq S_{ik}^{max} + \gamma_{ik}\ ,\ 0 \leq \gamma_{ik} \quad (17)$$

where the quantity S_{ik} is the apparent power through the line *ik* and ϵ_{ik} and γ_{ik} the variables of nonzero deviation if the initial constraints are not respected. For nodes, these are the tensions V_i, as gentle constraints. These voltages Vi are imposed to be around the reference value:

$$V_i^{min} \leq V_i^{ref} \leq V_i^{max}$$

$V_i^{min} = 0.95\, V_i^{ref}$ is the minimum acceptable value of the tension at the knot *i*;

$V_i^{max} = 1.05\, V_i^{ref}$ is the maximum acceptable value of the tension at the knot i.

For the static compensator of the reactive power, the reactive power QSVC can take the values included in the interval:

$$Q_{Cmax} \leq Q_{SVC} \leq Q_{Lmax}$$

If the static compensator of reactive power is of condensing type commutated by thyristor, only an injection of reactive power is possible and$Q_{Lmax} = 0$. The reactive power provided to the network is limited by:

$$0 \leq Q_{TSC} \leq Q_{Cmax}$$

If the static reactive power compensator is thyristor-switched capacitor type, only a reactive power injection is possible and Q_{Cmax} = 0. The reactive power supplied to the network is limited by:

$$0 \geq Q_{TCR} \geq Q_{Lmax}$$

The operating principle of the hybrid optimization method is given by the algorithm represented in Figure 5.

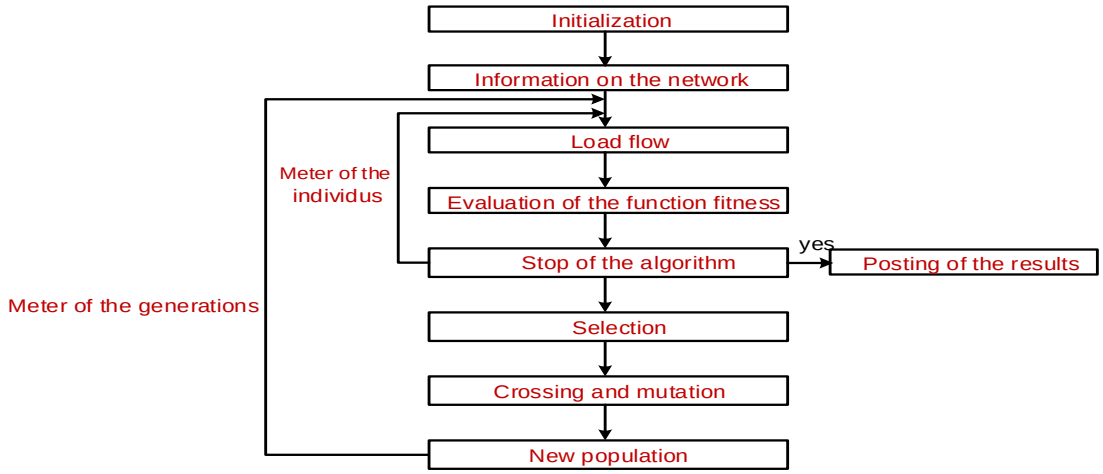

Figure 5: operation of the hybrid optimization algorithm.

3. Results and Discussion

The hybrid optimization method developed in this study is tested and applied to the interconnected Congolese electrical power network shown in Figure 6.

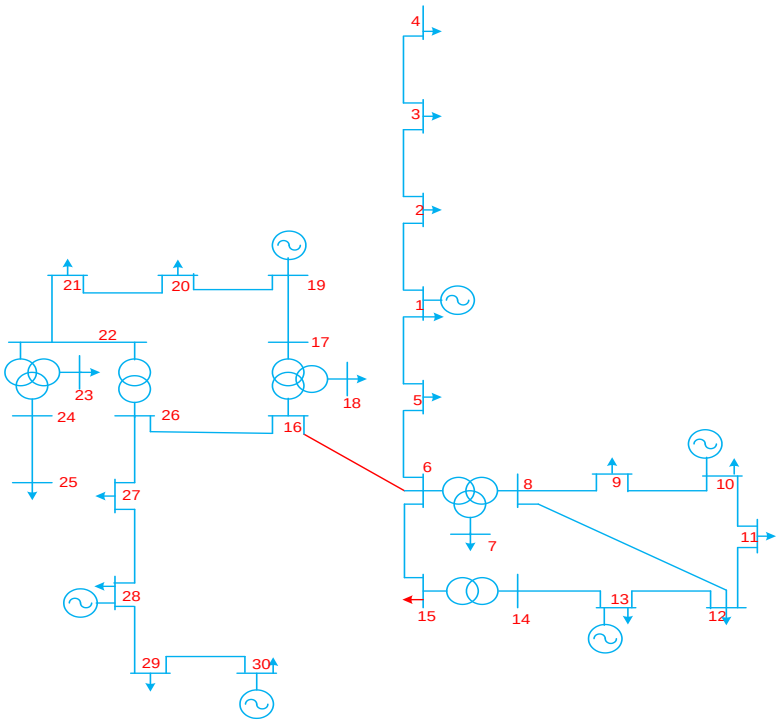

Figure 6: diagram of the Congolese electricity grid interconnected at 30 nodes.

3.1. Determination of stability limits

Using this method, we performed the simulations that allowed us to obtain the powers generated and consumed at the different nodes, ensuring the stability of the network in tension. Then the simulations when the total energy demand is served have made it possible to assess the degree of instability of the network in order to consider the compensation plan. The results of simulations are presented in Tables 1, 2, 3, 4 and 5 in the appendix and interpreted by the stress histograms of Figures 7 and 8.

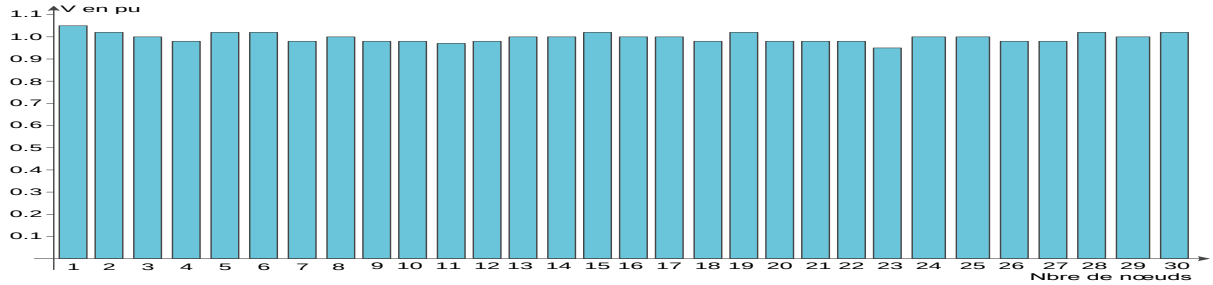

Figure 7: histogram of voltages when the stability of the network is respected.

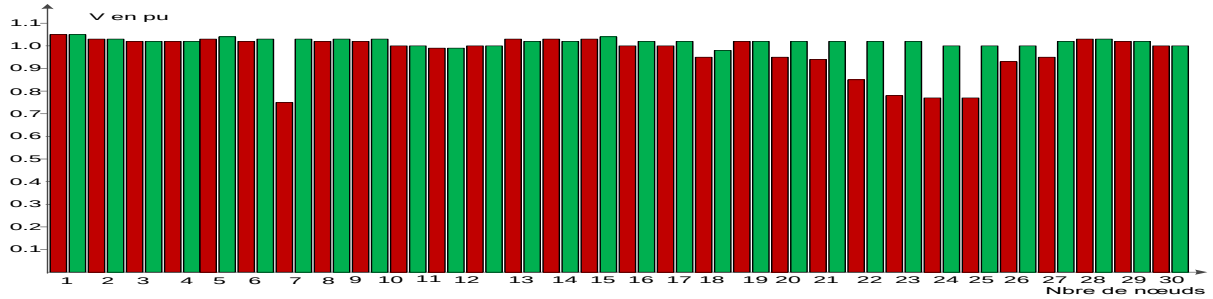

Figure 8: stick diagram of front voltages (in red) and after (in green) compensation.

Table 1: Phases and voltage magnitude, power injected or absorbed at the nodes when the voltage stability limits are respected.

n°	Phases in degree	Voltages V in pu	Power injected or absorbed in pu
01	0	1.0500	1.2015 + 1.0092i
02	-2.6075	1.0297	-0.2000 - 0.1240i
03	-4.9401	1.0101	-0.4500 - 0.2790i
04	-5.4072	1.0092	-0.1000 - 0.0620i
05	1.1107	1.0356	-0.4000 - 0.2480i
06	1.4601	1.0303	-0.0000 + 0.0000i
07	-4.0933	0.9588	-0.1000 - 0.0620i
08	0.7502	1.0160	-0.0000 - 0.0000i
09	0.7060	1.0088	*-0.1000 - 0.0620i*
10	0.9315	1.0200	0.3000 + 0.1657i
11	0.2695	0.9977	-0.1500 - 0.0930i
12	0.3108	1.0035	-0.0500 - 0.0310i
13	0.6671	1.0108	0.1500 - 0.0930i
14	0.6627	1.0107	-0.1000 - 0.1240i
15	1.3655	1.0284	-0.1000 - 0.0620i
16	5.2530	1.0126	0.0000 + 0.0000i
17	6.6496	1.0093	-0.0000 - 0.0000i
18	4.9766	0.9723	-0.1275 - 0.0790i
19	11.4108	1.0200	0.7200 - 0.0353i
20	10.4834	1.0021	-0.0500 - 0.0310i
21	10.2491	0.9980	-0.0500 - 0.0310i
22	9.5035	1.0014	0.0000 + 0.0000i
23	7.7342	0.9793	-0.0500 - 0.0310i
24	1.8990	1.0653	0.0000 + 0.0000i
25	1.4218	1.0663	-0.1000 - 0.0620i
26	13.3652	0.9814	0.0000 - 0.0000i
27	16.0928	0.9749	-2.0000 - 1.2400i

28	20.0166	1.0200	4.7500 + 2.7424i
29	18.2666	0.9933	-1.0000 - 0.6200i
30	17.6976	0.9849	0.5000 + 0.3100i

Table 2: Transited powers and losses in the lines when the voltage stability limits are respected

n°	sections	Power output line	Online losses
01	1-2	0.7613 + 0.1361i	0.0067 - 0.0824i
02	2-3	0.5546 + 0.0945i	0.0044 - 0.1106i
03	3-4	0.1001 - 0.0739i	0.0001 - 0.1359i
04	1-5	0.0403 + 0.6251i	0.0140 - 0.1460i
05	5-6	-0.3737 + 0.5230i	0.0014 - 0.0284i
06	6-7	0.1005 + 0.0767i	0.0005 + 0.0147i
07	6-8	0.0707 + 0.0756i	0.0001 + 0.0019i
08	6-15	0.1828 + 0.0989i	0.0001 - 0.0773i
09	8-9	0.0155 + 0.0307i	0.0001 + 0.0002i
10	8-12	0.0552 + 0.0429i	0.0004 + 0.0009i
11	9-10	-0.0846 - 0.0315i	0.0008 + 0.0007i
12	10-11	0.1146 + 0.0715i	0.0017 + 0.0027i
13	11-12	-0.0371 - 0.0243i	0.0002 + 0.0002i
14	12-13	-0.0325 - 0.0134i	0.0001 + 0.0001i
15	13-14	0.0174 - 0.1686i	0.0000 - 0.1813i
16	14-15	-0.0826 - 0.1112i	0.0000 + 0.0030i
17	6-16	-0.7292 + 0.3002i	0.0079 - 0.0227i
18	16-17	-0.4366 + 0.2305i	0.0041 + 0.0114i
19	16-26	-0.3004 + 0.0924i	0.0016 + 0.0286i
20	17-18	0.1299 + 0.0858i	0.0024 + 0.0068i
21	17-19	-0.5706 + 0.1332i	0.0156 + 0.0390i
22	19-20	0.1138 + 0.0466i	0.0012 - 0.0075i
23	20-21	0.0627 + 0.0231i	0.0002 - 0.0040i
24	21-22	0.0125 - 0.0039i	0.0000 + 0.0002i
25	22-23	0.0501 + 0.0333i	0.0001 + 0.0023i
26	22-24	0.1074 - 0.0935i	0.0073 + 0.0202i
27	22-26	-0.1451 + 0.0561i	0.0005 + 0.0108i
28	24-25	0.1001 - 0.1137i	0.0001 - 0.1757i
29	26-27	-0.4476 + 0.1091i	0.0038 - 0.0681i
30	27-28	-2.4515 - 1.0628i	0.0322 + 0.1969i
31	28-29	2.0163 + 1.3277i	0.0141 + 0.0811i
32	29-30	1.0023 + 0.6266i	0.0023 + 0.0066i
$\sum_{\substack{i=1 \\ j\neq 1}}^{n} \Delta \underline{S}_{ik}$			0.1243 – 0.6116i

Table 3: voltage phases and magnitude, powers injected or absorbed at the nodes before and after compensation

n°	Phases in degree		Voltages V in pu		Power injected or absorbed in pu	
	not compensated	compensated	not compensated	compensated	not compensated	compensated
01	0	0	1.0500	1.0500	1.1787 + 1.2197i	1.1425 + 1.0137i
02	-2.6075	-2.6075	1.0297	1.0297	-0.2000 - 0.1240i	-0.2000 - 0.1240i
03	-4.9401	-4.9401	1.0101	1.0101	-0.4500 - 0.2790i	-0.4500 - 0.2790i
04	-5.4072	-5.4072	1.0092	1.0092	-0.1000 - 0.0620i	-0.1000 - 0.0620i

05	1.4843	1.1784	1.0324	1.0373	-0.4000 - 0.2480i	-0.4000 - 0.2480i
06	1.8962	1.5670	1.0248	1.0322	0.0000 + 0.0000i	-0.0000 + 0.0000i
07	-15.7777	-11.8980	0.7682	1.0200	-0.2500 - 0.1550i	-0.2500 + 0.0256i
08	1.2376	0.8647	1.0146	1.0170	-0.0000 + 0.0000i	0.0000 + 0.0000i
09	1.2085	0.8388	1.0083	1.0091	-0.1000 - 0.0620i	-0.1000 - 0.0620i
10	1.4271	1.0863	1.0200	1.0200	0.3000 + 0.1615i	0.3000 + 0.1585i
11	0.7493	0.4082	0.9992	0.9983	-0.1500 - 0.0930i	-0.1500 - 0.0930i
12	0.7602	0.4312	1.0059	1.0044	-0.0500 - 0.0310i	-0.0500 - 0.0310i
13	1.0200	0.7739	1.0200	1.0123	0.1500 + 0.0180i	0.1500 - 0.0930i
14	1.0205	0.7694	1.0200	1.0123	-0.1000 - 0.1240i	-0.1000 - 0.1240i
15	1.7846	1.4728	1.0238	1.0302	-0.1000 - 0.0620i	-0.1000 - 0.0620i
16	6.7427	6.3980	1.0029	1.0150	0.0000 + 0.0000i	0.0000 + 0.0000i
17	7.8229	7.5970	1.0024	1.0113	0.0000 - 0.0000i	0.0000 - 0.0000i
18	6.1257	5.9308	0.9651	0.9744	-0.1275 - 0.0790i	-0.1275 - 0.0790i
19	11.6670	11.7992	1.0200	1.0200	0.7200 + 0.2200i	0.7200 - 0.1601i
20	10.5067	9.6325	0.9625	1.0200	-0.1360 - 0.0843i	-0.1360 + 0.1441i
21	10.4694	9.5664	0.9487	1.0131	-0.1000 - 0.0620i	-0.1000 - 0.0620i
22	13.1317	12.7619	0.8696	1.0093	-0.0000 + 0.0000i	0.0000 + 0.0000i
23	6.2514	7.9501	0.7905	1.0200	-0.1360 - 0.0843i	-0.1360 + 0.0307i
24	0.3178	2.9567	0.7697	1.0001	0.0000 + 0.0000i	-0.0000 - 0.0000i
25	-0.9562	2.1832	0.7612	0.9965	-0.1500 - 0.0930i	-0.1500 - 0.0930i
26	23.6459	21.7962	0.9374	1.0030	0.0000 - 0.0000i	0.0000 + 0.0000i
27	29.2737	26.8902	0.9627	1.0200	-2.0000 - 1.2400i	-2.0000 + 0.5575i
28	34.0347	31.8482	1.0200	1.0200	4.5000 + 2.5904i	4.5000 + 0.6332i
29	32.9077	30.7212	1.0031	1.0031	-0.8000 - 0.4960i	-0.8000 - 0.4960i
30	32.6297	30.4432	0.9990	0.9990	0.5000 + 0.3100i	0.5000 + 0.3100i

Table 4: Transited powers and losses in the lines before and after network compensation

n°	Sections	Power output line		Online losses	
		not compensated	compensated	not compensated	compensated
01	1-2	0.7613 + 0.1361i	0.7613 + 0.1361i	0.0067 - 0.0824i	0.0067 - 0.0824i
02	2-3	0.5546 + 0.0945i	0.5546 + 0.0945i	0.0044 - 0.1106i	0.0044 - 0.1106i
03	3-4	0.1001 - 0.0739i	0.1001 - 0.0739i	0.0001 - 0.1359i	0.0001 - 0.1359i
04	1-5	0.0174 + 0.8356i	-0.0188 + 0.6296i	0.0236 - 0.1393i	0.0142 - 0.1461i
05	5-6	-0.4062 + 0.7269i	-0.4329 + 0.5277i	0.0023 - 0.0247i	0.0015 - 0.0279i
06	6-7	0.2550 + 0.2983i	0.2521 + 0.0337i	0.0050 +0.1433i	0.0021 + 0.0593i
07	6-8	0.0646 + 0.0532i	0.0704 + 0.0802i	0.0000 +0.0013i	0.0001 + 0.0020i
08	6-15	0.1889 + 0.0092i	0.1832 + 0.1007i	0.0001 - 0.0767i	0.0001 - 0.0776i
09	8-9	0.0128 + 0.0272i	0.0152 + 0.0345i	0.0001 +0.0002i	0.0001 + 0.0003i
10	8-12	0.0518 + 0.0247i	0.0550 + 0.0437i	0.0002 +0.0006i	0.0004 + 0.0010i
11	9-10	-0.0873 - 0.0350i	-0.0849 - 0.0278i	0.0009 +0.0007i	0.0008 + 0.0007i
12	10-11	0.1119 + 0.0638i	0.1143 + 0.0681i	0.0015 +0.0025i	0.0017 + 0.0027i
13	11-12	-0.0397 - 0.0317i	-0.0373 - 0.0276i	0.0003 +0.0002i	0.0002 + 0.0002i
14	12-13	-0.0384 - 0.0388i	-0.0328 - 0.0160i	0.0004 +0.0006i	0.0002 + 0.0002i
15	13-14	0.0112 - 0.0833i	0.0170 - 0.1712i	0.0000 - 0.1847i	0.0000 - 0.1819i
16	14-15	-0.0888 - 0.0227i	-0.0830 - 0.1133i	0.0000 +0.0013i	0.0000 + 0.0030i
17	6-16	-0.9170 + 0.3909i	-0.9400 + 0.3410i	0.0127 +0.0109i	0.0125 + 0.0085i
18	16-17	-0.3460 + 0.1367i	-0.3710 + 0.2143i	0.0024 +0.0066i	0.0030 + 0.0086i
19	16-26	-0.5837 + 0.2432i	-0.5816 + 0.1182i	0.0067 +0.1695i	0.0057 + 0.1416i
20	17-18	0.1299 + 0.0859i	0.1299 + 0.0858i	0.0024 +0.0069i	0.0024 + 0.0068i

21	17-19	-0.4783 + 0.0442i	-0.5039 + 0.1199i	0.0106 +0.0241i	0.0121 + 0.0286i
22	19-20	0.2111 + 0.2277i	0.1840 - 0.0812i	0.0075 +0.0074i	0.0030 - 0.0035i
23	20-21	0.0676 + 0.1361i	0.0450 + 0.0664i	0.0009 - 0.0020i	0.0002 - 0.0040i
24	21-22	-0.0332 + 0.0760i	-0.0553 + 0.0084i	0.0004 +0.0078i	0.0002 + 0.0031i
25	22-23	0.1374 + 0.1100i	0.1367 - 0.0190i	0.0014 +0.0257i	0.0007 + 0.0117i
26	22-24	0.1644 + 0.0442i	0.1598 - 0.0336i	0.0138 +0.0383i	0.0094 + 0.0262i
27	22-26	-0.3355 - 0.0859i	-0.3518 + 0.0580i	0.0032 +0.0711i	0.0025 + 0.0560i
28	24-25	0.1506 + 0.0058i	0.1503 - 0.0598i	0.0006 - 0.0872i	0.0003 - 0.1528i
29	26-27	-0.9291 - 0.0833i	-0.9417 - 0.0214i	0.0163 +0.0092i	0.0146 - 0.0120i
30	27-28	-2.9453 - 1.3325i	-2.9563 + 0.5481i	0.0483 +0.3084i	0.0374 + 0.2318i
31	28-29	1.3063 + 0.8254i	1.3063 + 0.8254i	0.0058 +0.0246i	0.0058 + 0.0246i
32	29-30	0.5006 + 0.3049i	0.5006 + 0.3049i	0.0006 - 0.0051i	0.0006 - 0.0051i
$\sum_{\substack{i=1 \\ j\neq 1}}^{n} \Delta P_{ik}$				0.2130+0.2005i	0.1430 - 0.3231i

Table 5: Optimized nodes, optimized SVC reactive powers, and thyristor priming angles

n°	optimized nodes	Reactive power of the SVC in pu	Angle of ignition of thyristor in degree		
1	7	-0.1806	277.7758	or	- 82.2242
2	20	-0.2284	279.8906	or	- 80.1094
3	23	-0.1150	274.9045	or	- 85.0955
4	27	-0.5306	294.2542	or	- 65.7458

3.2. ATC determination

The Mindouli line - Tselampo (Brazzaville) or (6-16) has a capacity of 106,172 MVA per phase, of which 95,555 MVA = (81,221 + 50,3367i) MVA represents the 90% of the capacity that must not be exceeded, either (0.8122 + 0.50337i) pu. When locations 7, 20, 23 and 27 are taken into account, line 6-16 may pass (1.6861 - 0.5527i) pu or (0.562 - 0.1842i) pu per phase without violating the voltage stability limits. Since (0.9400 - 0.3410i) pu is the power demanded by Brazzaville, ie (0.3133-0.1137i) pu per phase when the system is assumed to be symmetrical or balanced, then: ATC = 0.2287 pu per phase, if the TRM and CBM components are neglected. Through this interconnection, the line can therefore transit 0.6861 or, if necessary and especially if there is availability. This statement is justified by the stability of the voltage network, since all the voltages at the various nodes of the network are within the limits provided by the standards. For example, for this operating regime, the lowest voltage is recorded at node 18 with a value of 0.9597 pu.

3.3. Discussion

The analysis of the histogram shown in figure 7 shows that, in order to guarantee the stable operation of the interconnected network of figure 6, the power transited in line 6-16 must be limited to (0.7292 - 0.3002i) pu.

However, the analysis of the histogram shown in figure 8 shows that, when the Brazzaville service in electrical energy is total, there are eight (8) nodes of instability of the network in tension, whose nodes seven (7), twenty-three (23), twenty-four (24) and twenty-five (25) are of extreme gravity, capable of driving the network to a collapse. Thus, the optimal locations of the four (4) SVCs respectively at nodes 7, 20, 23 and 27, generated by the hybrid optimization algorithm have allowed to reduce all the voltages in the standards.

Therefore, to guarantee the total coverage of Brazzaville and part of northern Congo, the power required to transit in line 6-16 at rush hour is (0.9400 - 0.3410i) pu. In addition, the losses joule went from 0.2130 pu before compensation to 0.1430 pu after compensation, representing respectively 3.89% and 1.94% of the total production.

4. Conclusion

The hybrid optimization method that we have just developed in this paper has made it possible, in the context of the harmonious management of meshed electrical networks, to optimize the location and susceptance of the SVCs or (the starting angle of the thyristor), in order to:

- stabilize the network in tension;
- reduce losses joule in the network;
- increase the transit capacity of the lines, a guarantee of the capacity available for transport.

However, the number of SVCs can be increased according to the financial possibilities of the company in order to further improve the results (good voltage performance of the network at higher transit capacities).

References

[1]. Lamia Kartobi. Optimization of the Synthesis of the FACTS by the Genetic Algorithms and the Particulate Swarms for the control of the Electrical communications. Memory of Magister November 2006. Polytechnic national school of Algiers.

[2]. N.G. Hingorani and L. Gyugyi, "Understanding FACTS", *IEEE Press.*, New York, 2000

[3]. Stephan Gerex; Metaheuristiques applied to the optimal placement of devices FACTS in an electrical communication. Thesis of doctorate, Federal Polytechnic school of Lausanne, 2003.

[4]. Nara K., "States of the Arts of the Modern Heuristics Applications to Power systems*", IEEE PES Winter Meeting*, January 2000, vol. 2, pp. 1279-1283.

[5]. K. Belacheheb. Contribution to the study of compensation systems FACTS in general, UPFC in particular, for the control of the transit of power in a grid system. Thesis of doctorate of the University of Henri Poincare Nancy I, June 21st, 2001.

[6]. Jean-Paul Barret, Pierre Bornard and Bruno Meyer. Simulation of the electrical communications. Eyrolles edition. 1997.

[7]. Jean-Claude Sabonnadiere and Nourédine Hadjssîd. Lines and electrical communications 2. Collection sciences and technologies of electrical energy 2008.

[8]. North American Electric Reliability Council: Available Transfer Capacity Working Group. Transmission Capability Margins and Their Use in ATC Determination. June 17, 1999.

[9]. Enrique Acha, Claudio R. Fuerte-Esquivel, Hugo Ambriz-Perez et César Angeles-Camacho. FACTS: Modelling and Simulation in Power Network. John Wiley & Sons LTD. December 2005.

[10]. Hans GlavitschL & Rainer Bacher. Optimal Power Flow Algorithms. Lecture Notes of Swiss Federal Institute of Technology. CH-8092 Zürich; Switzerland.

[11]. G. Glanmann, G. Aderson ETH Zurich. Using FACTS Devices to Resolve Congestions in Transmission Grids. ETH Zenturn, ETL G24.1, 8092 Zurich.